Ab Initio Method for Electromigration Analysis

H. Ceric[1,2], R. L. de Orio[2], W. H. Zisser[1,2], and S. Selberherr[2]
[1]Christian Doppler Laboratory for Reliability Issues in Microelectronics at the Institute for Microelectronics
[2]Institute for Microelectronics, TU Wien, Gußhausstraße 27-29, 1040 Wien, Austria
Phone: +431 No. 58801/36032 Fax: +431 No. 58801/36099 Email: Ceric@iue.tuwien.ac.at

***Abstract*-The reliability of interconnects in modern integrated circuits is determined by the magnitude and direction of the effective valence for electromigration (EM). The effective valence depends on local atomistic configurations of fast diffusivity paths such as metal interfaces, dislocations, and the grain boundary; therefore, microstructural variations lead to a statistically predictable behavior for the EM life time. Quantum mechanical investigations of EM have been carried out on an atomistic level in order to obtain numerically efficient methods for calculating the effective valence. The results of *ab initio* calculations of the effective valence have been used to parameterize the continuum level electromigration model and the kinetic Monte Carlo model. The impact of fast diffusivity paths on long term EM behavior is demonstrated with these models.**

I. Introduction

Electromigration (EM) experiments indicate that the copper interconnect lifetime decreases with every new interconnect generation. In particular, fast diffusivity paths cause a significant variation in the interconnect performance and EM degradation. In order to produce more reliable interconnects, the fast diffusivity paths must be addressed, when introducing new designs and materials. The EM lifetime depends on the variability of material properties at the microscopic and the atomistic level [1]. Microscopic properties are grain boundaries and grains with their crystal orientation. Atomistic properties are configurations of atoms at the grain boundaries, at the interfaces to the surrounding layers, and at the cross-section between grain boundaries and interfaces [2].
Modern Technology Computer-Aided Design (TCAD) tools, in order to meet the challenges of contemporary interconnects, must cover three major areas: physically based continuum modeling, *ab initio*/atomistic-level modeling, and statistical compact modeling.
The crucial parameter to predict the EM behavior is the effective valence which strongly differs between bulk, grain boundaries, dislocations, and interfaces. We present a computationally efficient *ab initio* method for calculation of the effective valence for EM and the atomistic EM force. The results of these *ab initio* calculation are applied for parameterization of a continuum-level model.

II. Theoretical Background and Analysis

Generally, the effective valence is a tensor field $\bar{Z}$, which defines a linear relationship between the EM force $\vec{F}$ and an external electric field $\vec{E}$.

$$\vec{F} = e\,\bar{Z}(\vec{R})\overrightarrow{E} \qquad (1)$$

For the calculation of the effective valence several methods have been proposed, all of them being based on the computation of electron scattering states [3]. Density functional theory (DFT), in connection with the augmented plane wave (APW) method [4] or the Korringa-Kohn-Rostoker (KKR) [5] method, has been established as the most powerful method for the determination of scattering states, however, it requires a demanding computational scheme. The cumbersome representation of scattering wave functions with many parameters represents a heavy burden on stability and accuracy of subsequent numerical steps. In this work we introduce a more robust and efficient method to calculate the effective valence, which relies only on the electron density $\rho(\vec{k},\vec{r})$.

The basic idea is presented in the following equations for the tensor components:

$$Z_{i,j}(\vec{R}) = \frac{\Omega}{4\,\pi^3}\iiint d^3\vec{k}\,\delta(\mathcal{E}_F - \mathcal{E}_{\vec{k}})\tau(\vec{k})\left[\vec{v}(\vec{k})\cdot\hat{x}_j\right]\times$$
$$\times\iiint d^3\vec{r}\;\rho(\vec{k},\vec{r})\left[\nabla_{\vec{R}}V(\vec{R}-\vec{r})\cdot\hat{x}_i\right]. \qquad (2)$$

V is the interaction potential between an electron and the migrating atom, $\tau(\vec{k})$ is the relaxation time due to scattering by phonons, $\vec{v}(\vec{k})$ is the electron group velocity, and Ω is the volume of a unit cell. The first integration is over the *k*-space and the second over the volume of the crystal. For the calculation of the electron density the DFT tool VASP [6] is used. An example of a VASP calculation is given in Fig. 1.

The electron density alone provides a qualitative explanation for the fact that the effective valence is higher in the bulk than in the grain boundaries. Similar analyses can be performed for atomic structures of different copper/insulator interfaces. Higher electron densities lead to higher effective valences, as can be seen from (2) [7]. For an accurate electron density calculation it is necessary to know the exact positions of the atoms in the structure.

The electric potential calculated with DFT is also applied for a simple jellium model. Here, the grain boundary is represented as a repulsive potential barrier for current carrying electrons. In this case the evaluation of integral (2) is not necessary, since

only a simple one-dimensional barrier problem must be dealt with, e.g. the precisely calculated DFT repulsive potential is approximated with a rectangular barrier potential. To estimate the value of the effective valence, both inside the grain boundary and in the copper bulk, an external electric field parallel to the grain boundary must be applied, obtaining the two-dimensional potential (cf. Fig.2). Current carrying electrons are now described with the two-dimensional Schrödinger equation

$$\frac{\hbar}{2m}\Delta_{x,y}\psi(x,y) + V(x,y)\psi(x,y) = \mathcal{E}\psi(x,y). \quad (3)$$

The two-dimensional potential can be separated into a component for the barrier $V(x)$ and a component due to the external electric field $V(y)$.

$$V(x,y) = V(x) + V(y) \quad (4)$$

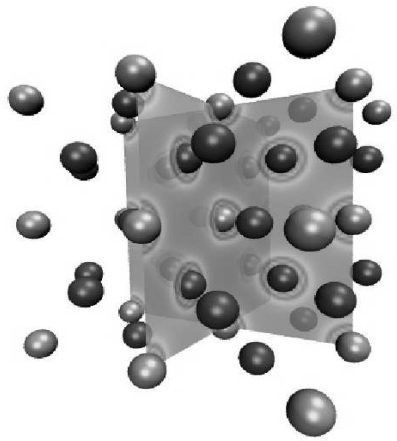

Fig. 1. Portion of the bulk copper crystal. The electron density is represented in two orthogonal planes. It varies from higher values (circle regions around atoms) closer to the atomic nucleus to lower in the inter-atomic space.

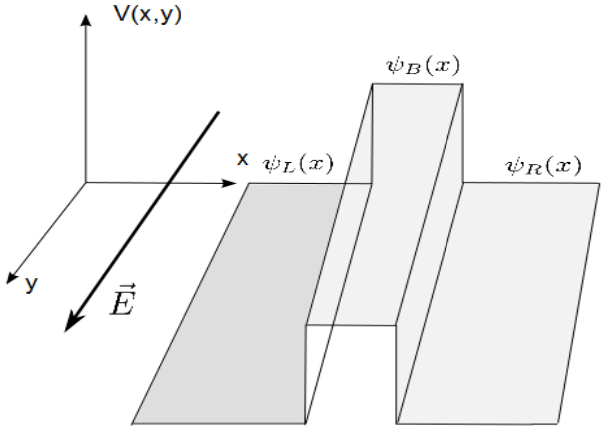

Fig. 2. Grain boundary represented by a two-dimensional potential barrier. In order to obtain the effective valence in the copper bulk and the grain boundary an external field oriented parallel to the grain boundary is utilized.

In this case, the solution of the two-dimensional Schrödinger equation is represented as a product of two one-dimensional solutions [8].

$$\psi(x,y) = \psi_x(x)\psi_y(y) \quad (5)$$

$\psi_x(x)$ is a usual potential barrier solution which is split into solutions $\psi_L(x)$, $\psi_B(x)$, and $\psi_R(x)$ for the region on the left side of the barrier, for the barrier region itself, and for the region on the right side of the barrier. $\psi_x(x)$ depends explicitly on the energy $\mathcal{E}$ and, therefore, the two-dimensional solution of the Schrödinger equation is denoted as $\psi(x,y;\mathcal{E})$. Electrons are accelerated in the external field $\vec{E}$ parallel to the grain boundary and thus $\psi_y(y)$ is given by the Airy function [8]

$$\psi_y(y) = Ai\left(\frac{y-\sigma}{\gamma}\right), \quad (6)$$

where

$$\gamma^3 = \frac{\hbar^2}{2me|\vec{E}|}, \quad (7)$$

and

$$\sigma = -\frac{\mathcal{E}}{e|\vec{E}|}. \quad (8)$$

The electron density $\rho(\vec{r})$ is easily calculated by integrating over the continuous energy states.

$$\rho(\vec{r}) = \int_0^\infty d\mathcal{E} f(\mathcal{E}-\mathcal{E}_F)\, DOS(\mathcal{E})|\psi(x,y;\mathcal{E})|^2 \quad (9)$$

Now, the electron wind force is given by a simpler expression [9]

$$\vec{F}(\vec{R}) = -\int d^3r\, \rho(\vec{r})\frac{\partial(\vec{r}-\vec{R})}{\partial\vec{R}}, \quad (10)$$

which is subsequently used in order to calculate the effective valence.

III. Kinetic Monte Carlo Simulation of Electromigration

To utilize results of quantum mechanical calculations for kinetic Monte Carlo simulations an average driving force along the diffusion jump path must be calculated. In general, the microscopic force-field will depend on the position of the defect along the diffusion jump-path.

The average of the microscopic force over the *j*-th diffusion jump path between locations $\vec{r}_{j,1}$ and $\vec{r}_{j,2}$ [3] is

$$F_{m,j} = \frac{1}{|\vec{r}_{j,1} - \vec{r}_{j,2}|} \int_{\vec{r}_{j,1}}^{\vec{r}_{j,2}} \vec{F}(\vec{r}) \cdot d\vec{r}. \qquad (11)$$

The change in diffusion barrier height $\Delta A_{\alpha,j}$ is equal to the net work by the microscopic force as the defect is moved from the initial to final sites over the entire jump path.
The rates of defect jumps were calculated using the harmonic approximation to transition state theory (TST) [10]. In this approximation the transition rate $\Gamma_{\alpha,j}$ is given by

$$\Gamma_{\alpha,j} = \nu_0 e^{-\frac{Em - \Delta A_{\alpha,j}}{kT}}. \qquad (12)$$

E_m is the migration energy (barrier) defined as the difference in energy between the transition state and the initial state, and ν_0 is an attempt frequency [10].
For each defect site □ the residence time is calculated as [11]

$$\tau_\alpha = \frac{1}{\sum_{j=1}^{k_\alpha} \Gamma_{\alpha,j}}. \qquad (13)$$

k_α is the number of possible jump sites from the site α. A single point defect is created at an arbitrary site, the clock is set to zero, and the defect is released to walk through the system. At each step, the jump direction is decided by a random number according to the local jump probabilities

$$P_{\alpha,j} = \tau_\alpha \Gamma_{\alpha,j}. \qquad (14)$$

The jump is implemented by updating the coordinates of the defect. By repeating the described random walk procedure for millions of defects, their concentration dependence on the effective valence tensor and the external field is calculated.

IV. Simulation Results and Discussion

The *ab initio* method described above is applied for the calculation of the effective valence inside grain boundaries and the calculated value is used to parameterize our continuum-level model [12]. Prior to carrying out the *ab initio* calculation it is necessary to construct grain boundaries with exact positions of atoms. For this purpose an in-house molecular dynamic (MD) simulator with a many-atom interatomic potential based on effective-medium theory [13] is used. The total energy of the system is expressed as

$$E_{tot} = \sum_{i=1}^{N} F(n_i) + \frac{1}{2} \sum_{i=1}^{N} \sum_{j \neq i} V(r_{ij}) \qquad (15)$$

for a *N*-atom system, where $V(r_{ij})$ describes a pair potential and $F(n_i)$ describes the energy due to the electron density. An example of the construction of grain boundaries by means of MD simulation is presented in Fig. 3.

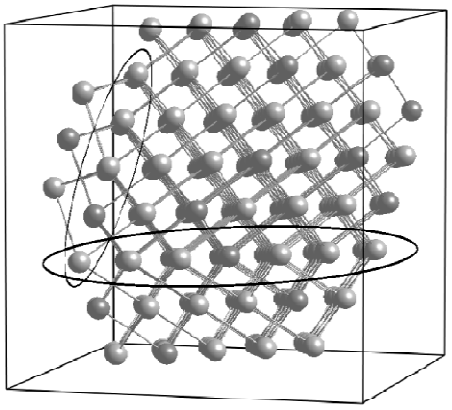

Fig. 3. Formation of grain boundaries (circled regions).

The electric potential inside the bulk and the grain boundary is calculated by means of DFT (cf. Fig. 4). Additionally the Fermi energy has been determined. The one-dimensional distribution of the effective valence is shown in Fig. 5. According to our calculation the effective valence inside the grain boundary is found to be 75% lower than in the bulk for a Fermi energy of 4.3 eV, a value which is in good agreement with the calculation of Sorbello [3].The calculated effective valence was set as a parameter in our continuum-level model [12]. For the same interconnect layout and operating conditions, three different copper microstructures exhibit three significantly different behaviors of EM driven vacancy transport (cf. Fig. 6) due to the variation of the effective valence between bulk and grain boundaries. The height of the vacancy concentration level in the quasi-equilibrium phase which starts about a second after the begin of the simulation differs for all three microstructures (cf. Fig. 6). However, the difference in the rapid phase of vacancy concentration growth, which starts about 1000 seconds later, is what makes an interconnect fail at significantly different times.

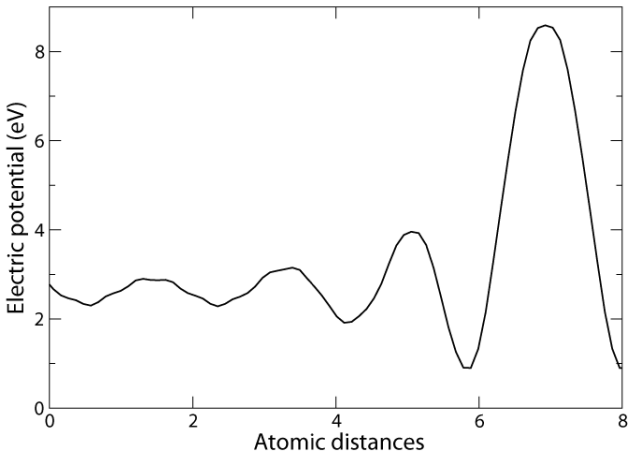

Fig. 4. Electric potential energy in the vicinity of the grain boundary and inside the grain boundary obtained by density functional theory.

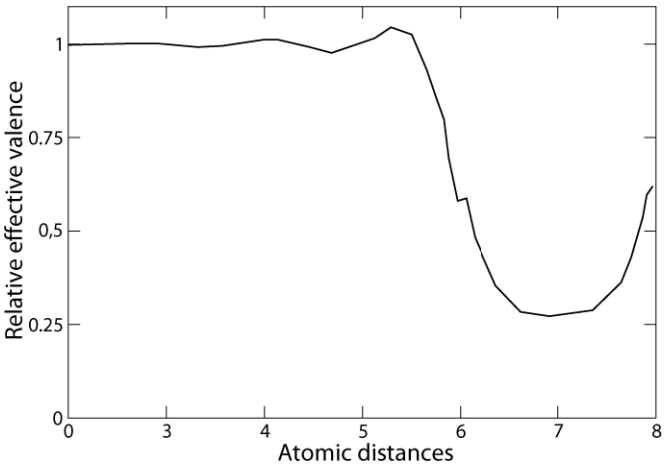

Fig. 5. Average distribution of the effective valence in x-direction near a grain boundary. The external electric field is oriented parallel to the grain boundary.

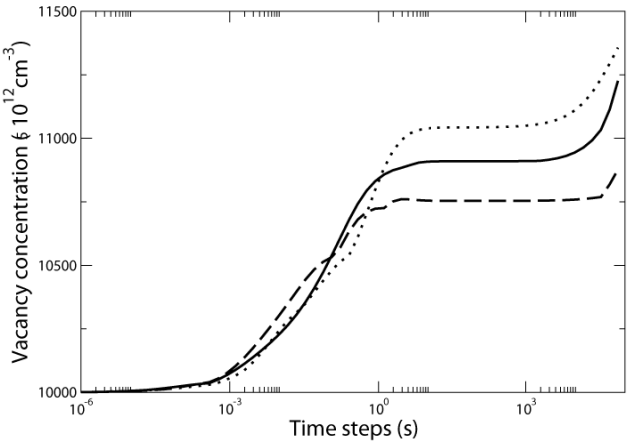

Fig. 6.Variation of the peak vacancy concentration with time for three different microstructures.

Along with the determination of the effective valence, ab initio calculations predict a lowering of the energy barrier for atomistic transport. Knowing the influence of the EM force on the diffusional barrier we utilize kinetic Monte Carlo [11],[14] simulations for EM, which provide a closer look into the distribution of atoms in the presence of EM for a specific atomistic configuration. The dependence of the atomic concentration on the angle between the EM force and the jump direction is displayed in Fig. 7. The EM intensity clearly reduces from $\theta = 0^\circ$, where the EM force acts in the fast diffusivity path direction, to a minimum for $\theta = 90^\circ$, where the EM force is orthogonal to this direction.

V. Conclusion

Our work introduces a novel approach for the calculation of the EM force on an atomistic level and demonstrates its application to continuum-level modeling. The consideration of the accurate effective valence in grain boundaries enables a realistic simulation of EM behavior. In addition, the presented combination of atomistic force calculations with a kinetic Monte Carlo simulation enables the sophisticated analysis of vacancy dynamics.

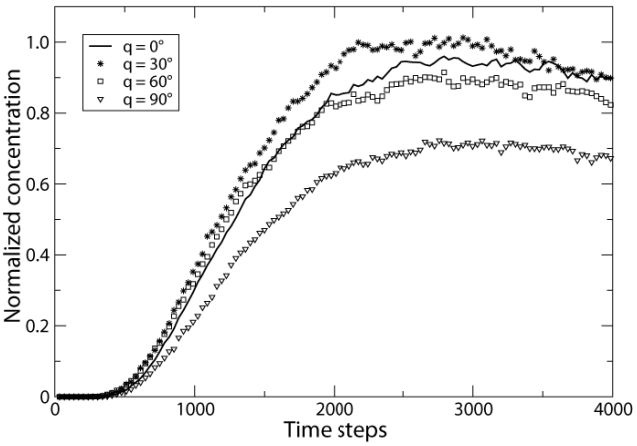

Fig. 7. Average distribution of the effective valence in x-direction near a grain boundary. The external electric field is oriented parallel to the grain boundary.

REFERENCES

[1] Z.-S. Choi, R. Mönig, and C. V. Thompsona, "Dependence of the Electromigration Flux on the Crystallographic Orientations of Different Grains in Polycrystalline Copper Interconnects," *Appl. Phys. Lett.*, vol. 90, p. 241913, 2007.

[2] E. Zschech and P. R. Besser, "Microstructure Characterization of Metal Interconnects and Barrier Layers: Status and Future," *Proc. Interconnect Technol. Conf*, pp. 233–235, 2000.

[3] R. S. Sorbello, "Microscopic Driving Forces for Electromigration," *Materials Reliability Issues in Microelectronics edited by J. R. Lloyd, F. G. Yost, and P. S. Ho*, vol. 225, pp. 3–10, 1996.

[4] R. P. Gupta, "Theory of Electromigration in Noble and Transition Metals," *Phys. Rev. B*, vol. 25, pp. 5188–5196, 1982.

[5] D. N. Bly and P. J. Rous, "Theoretical Study of the Electromigration Wind Force for Adatom Migration at Metal Surfaces," *Phys. Rev. B*, vol. 53, no. 20, pp. 13 909–13 920, 1996.

[6] G. Kresse and J. Furthmüller, "Efficient Iterative Schemes for *ab initio* Total-Energy Calculations Using a Plane-Wave Basis Set," *Phys. Rev. B*, vol. 54, no. 16, pp. 11 169–11 186, 1996.

[7] P. Kumar and R. S. Sorbello, "Linear-Response Theory of the Driving Forces for Electromigration," *Thin Solid Films*, vol. 25, pp. 25–35, 1975.

[8] R. W. Robinett, *Quantum Mechanics*. Oxford University Press, 1997.

[9] R. S. Sorbello, "Theory of Electromigration," *Solid State Phys.*, vol. 15, pp. 159–231, 1998.

[10] G. H. Vineyard, "Frequency Factors and Isotope Effects in Solid State Rate Processes," *J. Phys. Chem. Sol.*, vol. 3, no. 1, pp. 121–127, 1957.

[11] M. R. Sorensen, Y. Mishin, and A. F. Voter, "Diffusion Mechanisms in Cu Grain Boundaries," *Phys. Rev. B*, vol. 62, no. 6, pp. 3658–3673, 2000.

[12] H. Ceric, R. L. de Orio, J. Cervenka, and S. Selberherr, "A Comprehensive TCAD Approach for Assessing Electromigration Reliability of Modern Interconnects," *IEEE Trans. Dev. Mat.Rel.*, vol. 9, no. 1, pp. 9–19, 2009.

[13] H. Hakkinen and M. Manninen, "The Effective-Medium Theory Beyond the Nearest-Neighbour Interaction," *J. Phys. Condens. Matter.*, vol. 1, no. 48, pp. 9765–9777, 1989.

[14] G.E. Murch and I.V. Belova, "The Lattice Model for Addressing Phenomenological Diffusion Problems Associated with Grain Boundaries," *Interface Science*, vol. 11, pp. 91–97, 2003.